THE INTERDIGITAL MAGNETRON

BY

L. G. COLE

THE INTERDIGITAL MAGNETRON

-

L. G. Cole

THE INTERDIGITAL MAGNETRON

by

Lanier Guthridge Cole
Lieutenant, United States Navy

Submitted in partial fulfillment
of the requirements
for the degree of
MASTER OF SCIENCE

in

ENGINEERING ELECTRONICS

United States Naval Postgraduate School
Annapolis, Maryland
1951

This work is accepted as fulfilling
the thesis requirements for the degree of

MASTER OF SCIENCE

in

ENGINEERING ELECTRONICS

from the

United States Naval Postgraduate School

PREFACE

The preparation and writing of this thesis has taken place during the period from September 1950 to May 1951. During the first two years of the course in Electronics Engineering at the Postgraduate School and during the summer field trips, my attention was directed on numerous occasions to the fact that all sources of microwave energy are rather limited in their tuning range. It was decided to investigate the tuning of magnetrons and the possibilities of increasing their tuning range. In the course of this investigation and study, several articles on the interdigital magnetron were encountered. It was then decided to concentrate on an investigation of the possibilities of the interdigital magnetron as a source of broadband microwave energy. The results of this investigation are contained in this thesis.

During the time that the work on this thesis was being done, I was assigned to work at the Raytheon Manufacturing Company during the winter term. The suggestions and encouragement given during this time by Mr. J. Osepchuk and Mr. E. C. Dench of that company are gratefully acknowledged. The helpful comments of Professor W. P. Cunningham, who has followed this project from its inception, and Associate Professor A. Sheingold of the Staff are also gratefully acknowledged.

TABLE OF CONTENTS

TABLE OF CONTENTS

LIST OF ILLUSTRATIONS

CHAPTER I

INTRODUCTION AND EARLY HISTORY

Although the progress of microwave electronics has advanced greatly throughout the last decade, there is still one great limitation. That great limitation is the frequency sensitivity of most microwave components. Transmitters, receivers, duplexers and antennas are all narrow band devices as used today. In many applications this limitation is not serious, but in military electronics it is a limitation which should be overcome.

The seriousness of the problem from a military standpoint is threefold. First, there is the problem of detection of our radio and radar by the enemy. If our equipment is forced to operate on a fixed frequency, the chances of detection by the enemy go up tremendously, and the possibility of jamming by the enemy becomes much greater. Second, there is the problem of detecting the enemies' radio and radar. If each piece of intercept equipment can only cover a narrow band of frequencies, the number of equipments needed to search the frequency spectrum becomes excessive. Third, there is the problem of setting up equipments to jam the enemy. Again, we must have broad band jamming equipment in order to efficiently cover the frequency spectrum.

One element of this problem is the development of signal sources with a wide tuning range. Signal sources of both high and low powers are needed. The purpose of this

paper is to discuss and analyze the work which has been done with interdigital magnetrons. The possibilities and limitations of the interdigital magnetron as a solution to this problem will also be discussed. It is hoped that this paper in some small way may point the way toward the solution to this problem.

The interdigital magnetron or pill box cavity magnetron or donutron, as it has sometimes been called, is not new. In fact it really antidates the more successful and highly developed multicavity magnetron. The earliest reference to interdigital magnetrons is in 1938 in a paper by Gutton and Berline (4). Ludi (11) in 1940 examined the fields existing in interdigital structures. In this country several engineers, including Barrow and Dench at the Massachusetts Institute of Technology, were working on the interdigital magnetron when the British brought over the first successful multicavity magnetron. This magnetron was so far superior to any interdigital magnetron then available that all effort was concentrated on the multicavity magnetron. Some work, however, was done, and Dr. Benedict of Sylvania Electric Products, Incorporated produced a glass enclosed interdigital magnetron with an external tunable cavity (12). Since that time, work has been done by Crawford and Hare, Hull and Randals and research units at the University of Michigan and the University of Illinois. All of these developments will be discussed in a later chapter.

In the next chapter a general discussion of the inter-

digital magnetron, its modes of operation, and the fields which can exist therein will be given. The early developments in the field of interdigital magnetrons will be discussed in the third chapter. In the fourth chapter, a detailed mathematical analysis of the modes and fields existing in the interdigital magnetron will be given, and expressions for the mode wavelengths and external Q's will be derived. A discussion of operation in the zero order or cavity mode will be given in Chapter Five. Conclusions about the value of the interdigital magnetron as a possible solution to our problem will be drawn in the concluding chapter.

CHAPTER II

GENERAL DESCRIPTION AND THEORY OF OPERATION

1. Introduction

In the discussion of the interdigital magnetron, it will be presumed that the reader is familiar with the operation of the multicavity magnetron. The theory of operation of magnetrons is adequately covered by Fisk (3) and Collins (14). The interdigital magnetron operates in much the same way as the multicavity magnetron and obeys the same general laws. The only real difference is in the manner of obtaining the radio frequency fields. Hence, the discussion in this chapter will be limited to the types of fields which can exist in the interdigital structure.

The elementary interdigital magnetron (Fig. 1) consists of a cylindrical cavity which is closed at both ends. Extending in from each end surface is a set of fingers arranged in the form of a cylinder concentric with the cylindrical cavity. The two sets of fingers thus formed are interleaved one with the other without touching. The cathode is placed axially in the center of this tooth structure.

Thus we have an N-fingered anode with a single resonant cavity in place of the N-pole anode consisting of N identical, mutually coupled oscillating cavities of the multicavity magnetron. The interdigital magnetron has several modes of operation, but they are more widely spaced in frequency than in the multicavity magnetron. This can be attributed to the

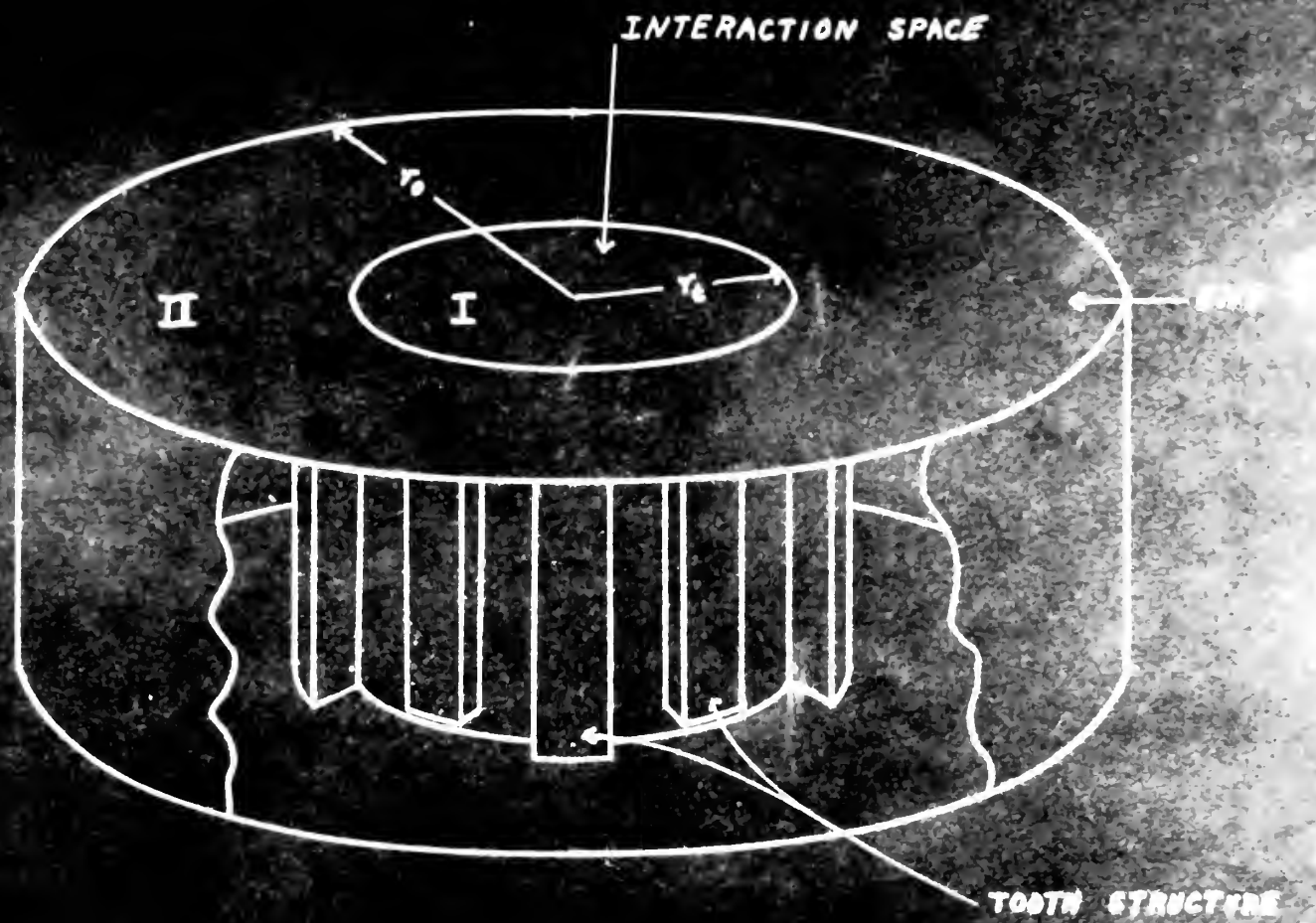

FIG. 1 - INTERDIGITAL MAGNETRON CAVITY

single resonant cavity as well as to the fact that the interdigital magnetron is a heavily strapped structure.

The fields which exist in the various modes will be given, and drawings will be given of the electric and magnetic field distribution as well as the current distribution in the zero order cavity mode and the first order mode. In these drawings the arrows with solid barbs indicate the current flow while the arrows with open barbs indicate the electric field. The magnetic field lines are show as dotted lines. The local fields at the tooth structure are neglected, and the cathode is assumed to be absent.

It will be shown in Chapter Three that the E_z, H_r and H_ϕ fields vary with the cosine or sine of $n\phi$, where n is the mode number, and vary radially as the sum of Bessel functions of the first and second kind. There are no variations in the z-direction.

2. Cavity Mode (n=o)

Fig. 2(a) shows the currents on one of the end surfaces of the cavity. The currents in the opposite end are in the opposite direction. It can be seen that the magnetic field lines are concentric with the axis and are independent of z and ϕ. Fig. 2(b) shows the currents and fields in a cross-sectional view. Fig. 2(c) shows the currents in a rolled out view of the anode as seen from the axis. One of the important features of the cavity mode is that the current and potential distributions do not vary with angular displacement, and the lines of magnetic flux within the cavity

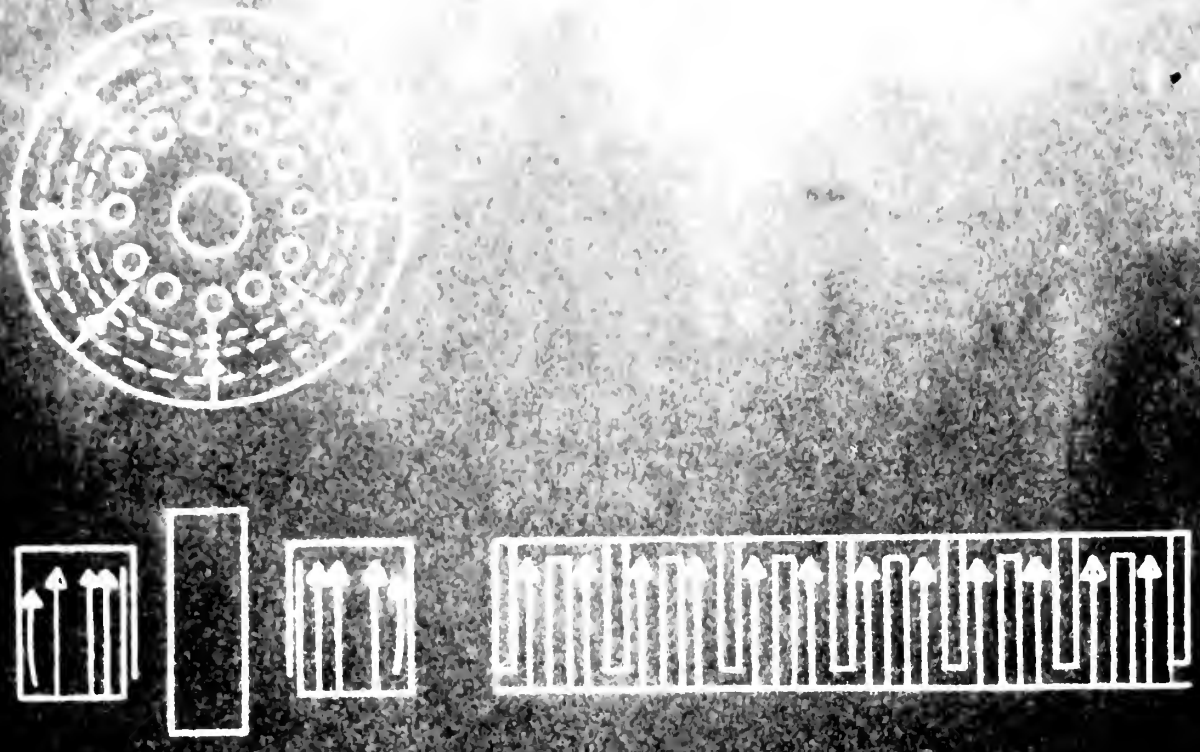

FIG. 2 FIELDS IN THE CAVITY MODE

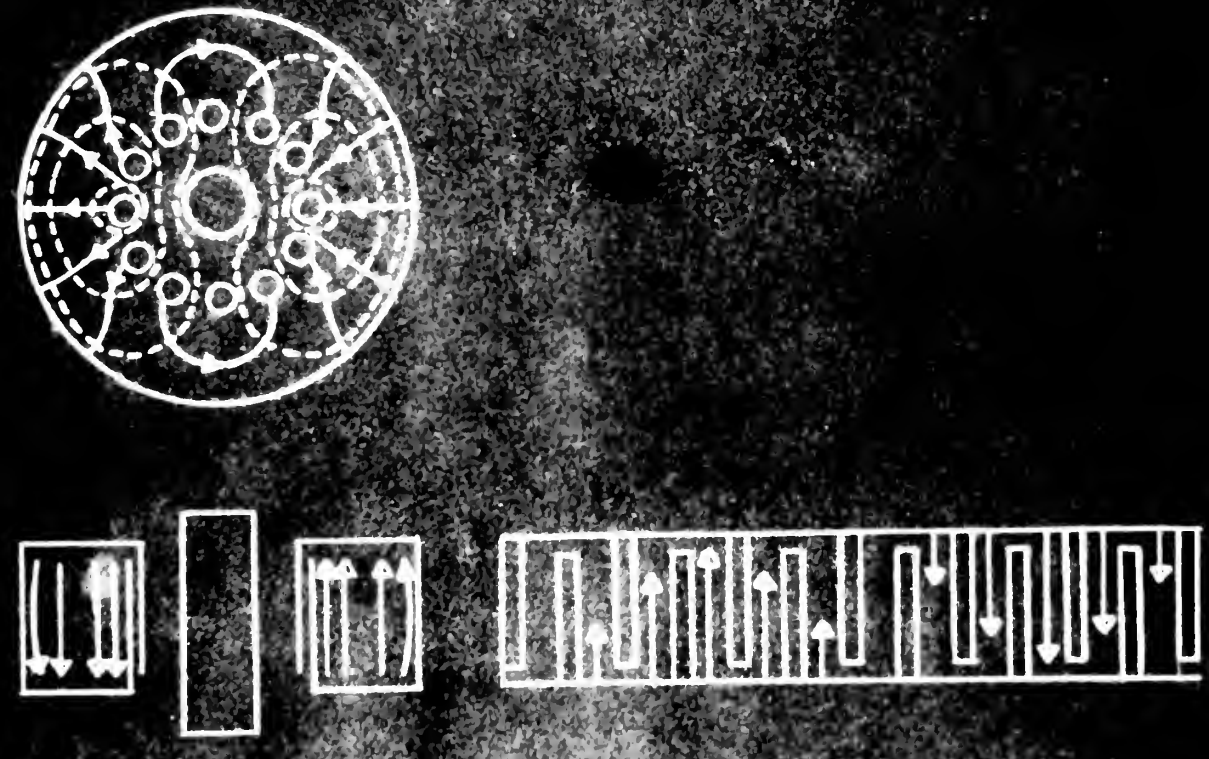

FIG. 3 FIELDS IN THE FIRST ORDER MODE

do not thread through the tooth structure. The fingers alternate in polarity and the magnitude of the voltage between them is invariant with angle. Thus an uncontaminated π-mode configuration is presented to the cathode. In this mode the cavity is the principal source of oscillations and its frequency is determined by its dimensions and by the capacitance of the teeth which is shunted across it.

Crawford and Hare (1) have taken probe patterns of the various modes of the interdigital magnetrons. These probe patterns show the square of the radial electric field strength as a function of angle. The probe pattern for the cavity mode in an anode having 16 fingers is shown in Fig. 4. In this probe pattern, there is no variation in the envelope of the probe pattern as we progress around the anode. There are variations due to the alternating charge on the fingers of the anode. Here, the number of fluctuations is equal to the number of teeth.

3. First Order Mode (n=1)

Fig. 3(a) shows the current flow on one end surface of the cavity. The currents on the opposite end surface are in the opposite direction at corresponding points. Fig. 3(b) shows the currents and fields in a cross sectional view. Fig. 3(c) shows the currents and potentials on the anode in a rolled out view as seen from the cathode. As can be seen, all fields vary sinusoidally with ϕ. It can be seen that the magnetic field threads through the tooth structure. Thus we might expect that the tooth structure would display some

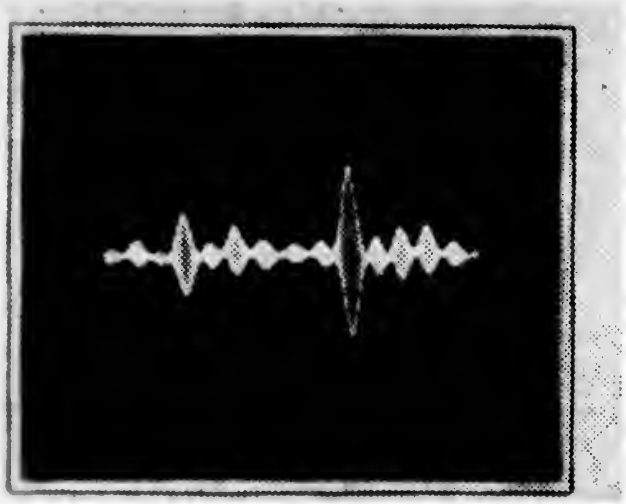

Fig. 5 Probe Pattern in the First Order Mode

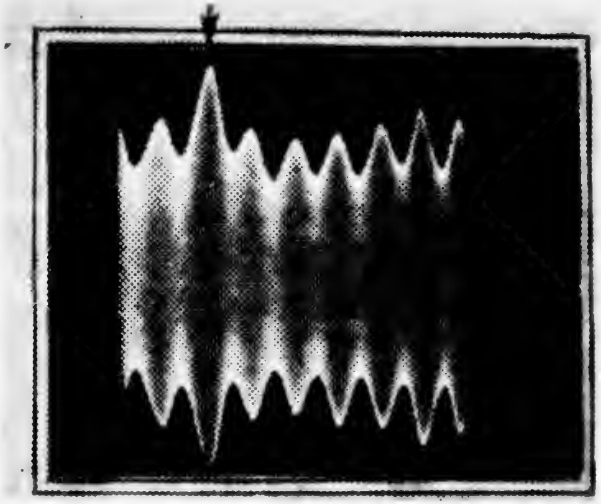

Fig. 4 Probe Pattern in the Cavity Mode

resonance phenomena of its own, and hence help to determine the resonant frequency of the anode structure. As it turns out, the tooth structure is the dominant resonant circuit in this mode, and the cavity is forced to oscillate as an odd quarter wavelength radial line.

Fig. 5 shows the probe pattern for this mode as observed by Crawford and Hare. Here we see that the envelope of the probe pattern is sin ϕ, and we again have the fluctuations due to the alternating charges on the teeth of the anode. This indicates that there is a single standing wave around the circumference of the anode.

It was observed at this time that the resonant wavelength was relatively independent of the cavity dimensions. This led to an empirical formula for the resonant wavelength in this mode which was based on the fact that the tooth structure seemed to resemble a folded two-wire re-entrant transmission line. This equation will be given in Chapter IV.

4. Higher Order Modes (n>1)

The fields and currents in the higher order modes are similar to the fields and currents in the first order mode except that the fields have n-variations around the anode. However, they are not very important as the efficiency in these modes is low.

5. Higher Order Radial Modes

In addition to the previously mentioned modes which have various azimuthal variations, there are some modes

which have nodes at various radial distances. All of these higher order modes, whether they be of radial or azimuthal variation, occur at higher frequencies than the basic cavity mode. The frequency mode separation from the basic cavity mode is greatest for the higher order radial modes.

CHAPTER III

EARLY DEVELOPMENTS OF INTERDIGITAL MAGNETRONS

1. Early French Magnetron

In 1938, H. Gutton and S. Berline (4) designed and built a magnetron of the interdigital type. This magnetron consisted of a cathode placed inside of a series of anode segments. These anode segments projected alternately from each end of a cylindrical structure. Fastened to each end of this arrangement was a shorting ring. A power output of about 7 watts with an efficiency of 15% at wavelengths between 10 and 20 cm. was obtained. No data on the mode of operation is available.

2. Resonant Cavity Magnetron

In 1939, Dr. W. L. Barrow of the Massachusetts Institute of Technology proposed and supervised the design and construction of a resonant cavity magnetron. The design and construction was carried out by Mr. Edward C. Dench (2) as a graduate student at the Massachusetts Institute of Technology. This work was completed in May of 1940.

The tubes which were constructed were of the interdigital type, having a small number of teeth. Tubes having two and four teeth were built and operated successfully. Nickel was used as the anode and cavity material in most of the tubes. The filament was of tungsten wire while the entire tube was enclosed in a glass envelope. The power was coupled out by means of a loop to a two wire transmission

line. The power was measured by means of an incandescent lamp and a photometer, and hence the power output measurements are probably inaccurate.

Large scale models of the tubes were built and cold test measurements made. It was noted that frequency decreased with increase in finger length. It was also found that no indication of resonance could be obtained when the cathode was inserted. It was believed that this was due to the fact that the filament acted as an antenna to couple the power out of the cavity. In order to verify this hypothesis, the filament was used as the input probe and positive indications of resonance were obtained. An attempt was made at this time to calculate the resonant frequency, but these attempts met with little success.

The cavity dimensions and tooth structure radii were the same for all the tubes built. The cavity diameter was 3 cm. and the cavity height was also 3 cm. The tooth structure radius was .5 cm. The tooth overlap was 1.5 cm.

The tubes were operated primarily in the cavity mode, but operation was noted in some of the higher order modes. When operating in the cavity mode, the wavelength for the two-tooth tubes was about 15 cm. whereas, for the four-tooth tubes, it was about 11 cm. Operation in the higher order modes was noted at wavelengths as short as 5 cm. The maximum power output obtained was 6.6 watts of CW power at 16.6% efficiency. Power output was limited both by back bombardment of the cathode and by anode dissipation.

Since this was one of the earliest, if not the earliest attempt to use a resonant cavity as the oscillating circuit in a magnetron, the recommendations made at that time are of interest. These were: Investigation of space charge effects with a view toward increasing the efficiency; Reduction of filament radiation by altering the filament-to-resonator capacity; Reduction of back bombardment power: use of low loss glass and elimination of the glass envelope; Use of coaxial or waveguide outputs; Use of copper or silver as the anode material; Improvement of power measuring methods; and Study of optimum tube dimensions; most of these recommendations have been carried out and have been proved successful.

3. Separate Cavity Tunable Magnetron

During World War II, Dr. Donald L. Benedict and Francis C. Breeden of the Research Laboratory of the Sylvania Electric Products, Incorporated worked on and developed an operable interdigital magnetron. In this magnetron, the tooth structure was fixed, while the cavity was tunable.

This tube (Fig. 6) was of the disc seal type. The two discs are separated by a glass cylinder and the ends are sealed by glass cups. Lead-in wires for the cathode and heater are brought through one of the glass cups. The teeth are inside the tube and are attached to the two end discs as shown in the elementary interdigital magnetron, Fig. 1. The cathode is placed in the center of the tube. An external cavity is screwed onto the discs to complete the tube. The

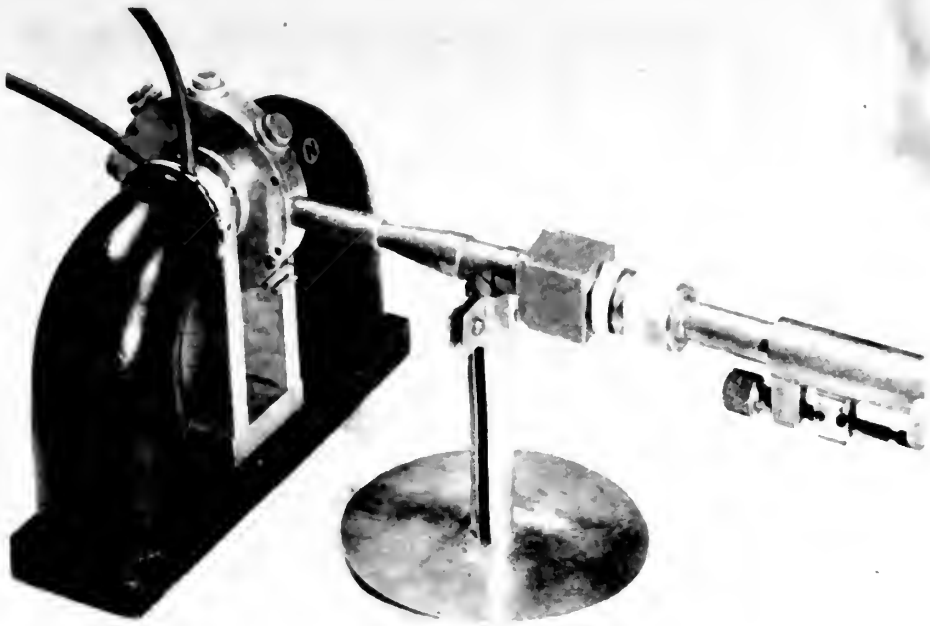

Fig. 7 Separate Cavity Interdigital Magnetron with Magnet

Fig. 6 Separate Cavity Interdigital Magnetron

external cavity is tuned by means of tuning plugs. The tube is mounted in a permanent magnet with the lines of magnetic force running along the axis of the tube. A tube mounted in its permanent magnet is shown in Fig. 7.

This tube was designed for Pulse Time Modulation communications equipment operating on a wavelength of 6 cm. The amplitude of the voltage pulses applied to the tube was 1500 volts at a 10% duty cycle. The pulse duration was 4 sec. and the magnetic field strength was about 1000 gauss. The peak power output of the tube was about 80 watts at 10% anode efficiency.

Although the analysis of its operation given in the literature is rather sketchy, it appears that the tube operated in the first order mode with the cavity oscillating as a three-quarter wavelength radial line. The three-quarter wavelength line was necessary to allow for the space taken by the glass cylinder. This also permitted placing the glass approximately at a voltage node so as to reduce losses in the glass.

In this tube, the cavity could be held fixed while the rest of the tube could be rotated. When this was done, it was found that there were two places where the power output was a minimum as well as two places where the power output was a maximum. It was found that if the cathode were mounted off center, the minimums were approximately zero, and the maximums of power were greatest. This enabled the tube to be mounted in a position such that maximum power was obtained.

A discussion of this effect will not be made at this time, but will be made later when the developments of Crawford and Hare are discussed.

The operation of this tube was good over a fairly wide range of frequencies. One value of anode voltage and magnetic field intensity was used over the range of operation. The pushing figure of the magnetron was also considered good.

4. The Donutron

F. H. Crawford and M. D. Hare (5) of the Radio Research Laboratory have constructed an interdigital magnetron which they have termed the donutron. The donutron as developed by them is tuned by leaving the cavity fixed while varying the tooth structure. In addition to constructing the tubes, they performed some interesting experiments which are of value in understanding the operation of interdigital magnetrons. Some of the results of their study of the fields by means of probe patterns in the interdigital structure were discussed in the preceding chapter.

The construction of the donutron is quite like the elementary interdigital magnetron shown in Fig. 1. One of the end surfaces was constructed as a thin diaphragm. This enabled the separation between the two end surfaces to be changed. This primarily changed the capacitance between the teeth, and hence tuned the tube. Various devices for accentuating the change in capacitance were tried. Among these were radial tabs or finger nails on the ends of the fingers, and circumferential rings attached to the fingers

belonging to a common anode half.

Inasmuch as the probe patterns indicated that an uncontaminated pi-mode field configuration was presented to the cathode in the cavity mode, it was decided to attempt to operate the tube in this mode. In addition it was noted that the tuning range observed on cold test was adequate. When the tube was placed on hot test, it operated in the cavity mode at low currents, but as the current was increased, it jumped into the first order mode. The maximum power output obtained before this mode jump occured was 10 watts at 35 per cent efficiency. This tube as well as all the others constructed by Crawford and Hare was operated as a CW tube. Tuning ranges of about 1.3 to 1 were obtained with plain fingers. The addition of finger nails or rings increased this range to 1.7 to 1 or higher. Because of this mode jump it was decided to concentrate on operation in the first order mode.

Crawford and Hare, realizing that the π-mode field configuration is the most efficient type of field configuration, investigated the fields existing in the first order mode with a view toward obtaining an approximation of the π-mode field. As the result of this investigation an anode with phase-reversing teeth was developed.

The best way of showing the necessity for phase-reversing teeth and of showing the effects of these teeth on the field configuration is by reference to a diagram such as Fig. 8. In Fig. 8(a), we see a simple anode rolled out in

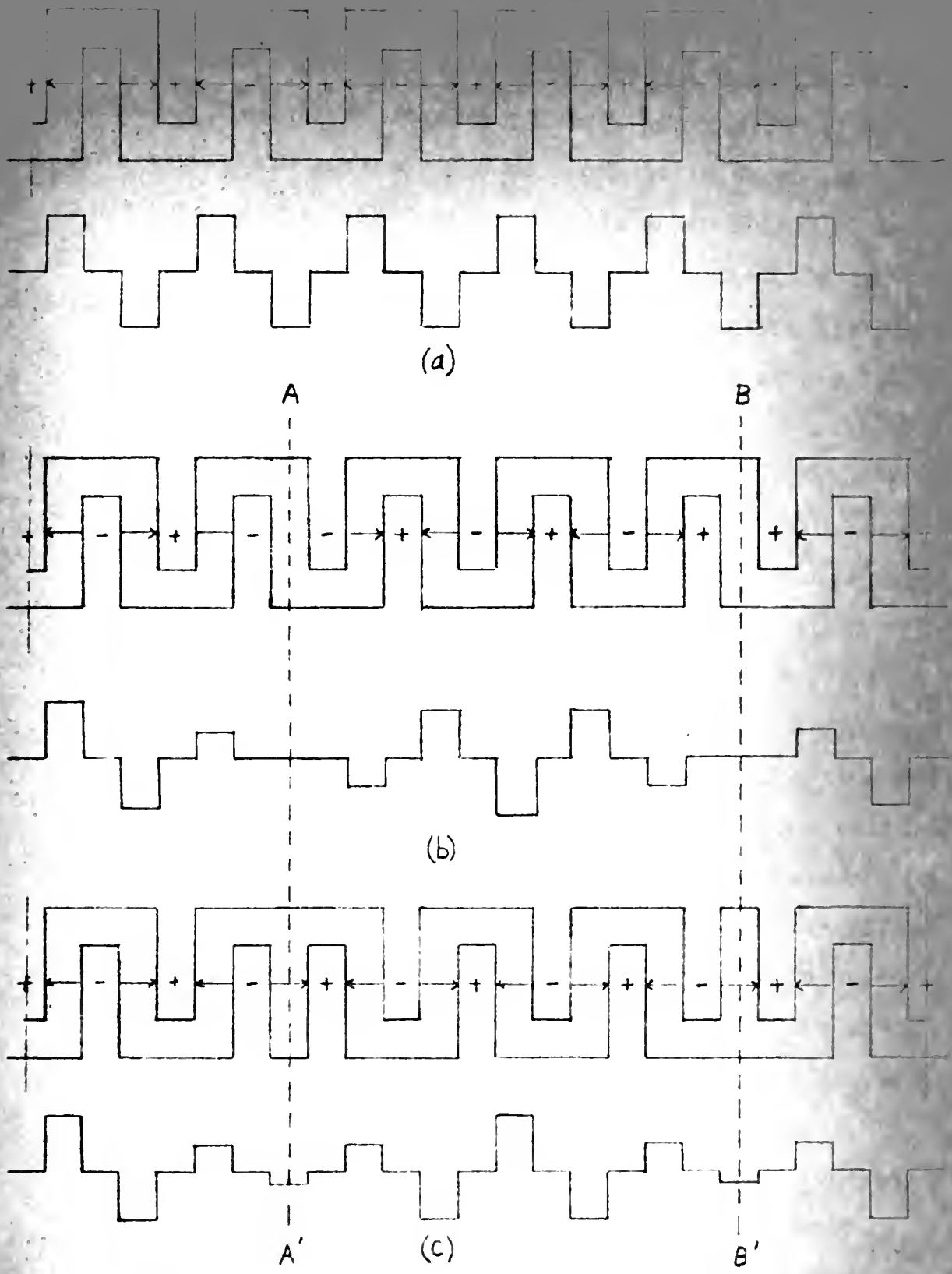

FIG. 8 - DIRECTION AND VARIATION OF THE AZIMUTHAL COMPONENT OF ELECTRIC FIELD FOR INTERDIGITAL ANODES.

(T) ANODE STRUCTURE

(F) ELECTRIC FIELD AT MID-SECTION

a plane. Beneath it is shown the field seen by the cathode in the cavity mode. Here, we have a simple regularly alternating field of constant amplitude. In Fig. 8(b), we again have a simple anode. Underneath it is shown the field seen by the cathode in the first order mode. This field is obtained simply by multiplying the field in the cavity mode by sin ϕ. Here we have an alternating field of varying amplitude, but the alternations are no longer regular. The fields between the nodal lines A-A' and B-B' are reversed from those of the cavity mode. Now, if we take the fingers between the nodal lines and shift them from one end surface to the other end surface, we have the rolled-out anode shown in Fig. 8(c). Below it is shown the field configuration now seen by the cathode in the first order mode. Here, the field alternates regularly as in the cavity mode, but has a variation in amplitude. The two teeth, at the nodal lines attached to the same anode half, may be left as one broad tooth since the voltage between them is small. This situation, which requires phase-shifting teeth, obtains whether the number of teeth be an even or odd multiple of two. If the number of teeth is an even multiple of two, the phase-reversing teeth are attached to different anode halves and the anode halves are identical. If, however, the number of teeth is an odd multiple of two, the phase-reversing teeth are attached to the same anode half and each anode half is symmetrical for ease in hand milling of the anode halves.

Upon investigating the first order mode more closely, it was found that two modes existed at nearly the same frequency. These two modes have nodal planes at right angles to each other. If the anode and cathode were perfectly symmetrical, these modes would be degenerate. If the structure is unsymmetrical, the modes are fixed in position and become less degenerate. This helps to explain the variation of power with azimuthal angle noted by the Sylvania group. If we call the mode which is directly coupled to the loop, the black mode, and the other mode which is indirectly coupled to the loop through intermode coupling, the red mode, we can differentiate between the two modes in this discussion.

The existence of the somewhat degenerate red mode at nearly the same frequency as the black mode is very undesirable in this mode of operation. This is due to the fact that, when the anode voltage and the magnetic field are adjusted for operation in the black mode, the red mode is also excited. The red mode thus subtracts power from the source and dissipates it as heat in the anode.

One of the general methods of preventing the excitation of an unwanted mode is to detune that mode from the frequency of the desired mode. In the interdigital magnetron, this may be done in several ways. The presence of phase-shifting teeth helps to eliminate the unwanted mode. Since the phase-shifting teeth are at a node for the black mode, they are at a voltage loop for the red mode. Hence, increas-

ing the capacitance at the phase shifting teeth will decrease the frequency of the red mode considerably while leaving the black mode frequency relatively constant. This may be done by adding wide fingers to the outside of that half of the amode which does not have the phase-shifting teeth. If finger nails or tabs are put on all of the teeth but the phase-shifting teeth, the black mode is shifted to a higher frequency than the red mode.

Operation in the first order mode was satisfactory using the improvements mentioned above. A CW power output of 50 watts at 40 to 50% efficiency was obtained. The tuning ranges attained were 1.5 to 1 or higher. This tuning range was limited by the fact that when the teeth were brought close together, a number of closely spaced "millimeter" modes were observed. This trouble seemed to be eased by the precise alignment of the anode halves and by use of a precision tuner. The power output was fairly constant throughout the tuning range with the use of a single value of anode voltage and magnetic field.

CHAPTER IV

WAVELENGTH AND Q EQUATIONS

1. Introduction

In any discussion of the Interdigital Magnetron, a knowledge of the mode wavelengths and the Q values to be expected are essential. Hull and Greenwald (9) have derived equations for the mode wavelengths and Q for an interdigital magnetron. The procedure as used by Hull and Greenwald will be used in the derivation shown below. The steps in the derivations will be carried out in greater detail, errors will be corrected, and the derivation of the wavelength formula when the end spaces are completely closed will be carried out.

Lucke (10) has derived an equation for the mode wavelengths using a slightly different approach. Some of the more interesting points will be given and it will be shown that the wavelength equations of Hull and Greenwald (9) and Lucke (10) are equivalent.

2. Symbol Definitions

All symbols used in this paper and not listed here are standard in mks system of units. All quantities used here are in rationalized mks units.

k_1 - $2\pi/\lambda$

r_o - radius of outer cylindrical wall of cavity

r_t - mean radius of tooth structure

$\propto$ - number of teeth

Δr - radical tooth thickness

$\Delta\phi$ - angle between adjacent teeth surfaces

d - axial length of the cavity from one end surface to the other

c - total equivalent capacitance between adjacent teeth in the tooth structure per tooth

n - mode number of the sinusoidal variations of the fields around the cavity

S - loop area

$H_{\phi 0}$ - magnetic field intensity at the outer cylindrical wall (rms) (at location of the loop)

V_1 - induced loop voltage (rms)

L - loop inductance

I_1 - loop current (rms)

Z_o - characteristic impedance of output loop

a - numerical coefficient which is equal to 2 when $n = 0$ and is equal to 1 when $n > 0$

ϕ_1 - angle between output loop and current max.

M - fraction by which the radial component of magnetic flux is constricted as it threads through the tooth structure. M is equal to the ratio of the total area of the tooth structure between surfaces at the mean tooth structure radius to the total area of the apertures between teeth.

ξ - factor by which the true capacitance between teeth is greater than the capacitance calculated when fringing is neglected.

G - see description after eq. 4.9

A,B,D - field amplitude-determining constants which cancel

out in resonant wavelength and external Q calculations.

3. Fields in the Interdigital Magnetron

Fig. 1 is an interdigital magnetron cavity of the conventional type. All principal dimensions and the general structure of the cavity are shown. In this derivation r_t and d will be assumed less than a half free-space resonant wavelength. It will also be assumed that the number of teeth is much greater than the mode number, that the teeth are very thin, and that the cathode is absent.

The problem will be solved by setting up the field equations in the two regions of the magnetron. Region I is the region inside the tooth structure ($0 < r < r_t$). Region II is the region between the tooth structure and outer cylindrical wall ($r_t < r < r_o$). The fields in the two regions are matched at the tooth structures and the currents in the tooth structure, induced by the magnetic field, are equated to the capacitive currents in the tooth structure, due to the electric field.

Lucke (10) has shown that the dominant modes of an interdigital magnetron under the assumptions given above are TM-modes of no z-variation. All other modes decay rapidly in the vicinity of the obstacle. Hence only TM-modes of no z-variation will be considered in the derivation. For these dominant modes the following equations from pp. 326-7 of Ramo and Whinnery (13) are used. (γ has been set equal to zero to give no variation in the z direction).

$$E_z = R\,F(\phi)\,e^{j\omega t} \tag{4.1}$$

$$F(\phi) = D\cos(n\phi) \tag{4.2}$$

$$R = A\,J_n(K_1 r) + B N_n(K_1 r) \tag{4.3}$$

$$H_r = \frac{1}{K_1^2}\left(\frac{j\omega\varepsilon_1}{r}\frac{\partial E_z}{\partial \phi}\right) \tag{4.4}$$

$$H_\phi = -\frac{1}{K_1^2}\left(j\omega\varepsilon_1 \frac{\partial E_z}{\partial r}\right) \tag{4.5}$$

$$K_1^2 = \omega^2 \mu_1 \varepsilon_1 \tag{4.6}$$

4. Fields in Region I

Since $N_n(K_1)$ becomes infinite as r approaches zero, the coefficient B_1 must be equal to zero and the fields in Region I become:

$$E_{z_1} = A_1 D_1 \cos(n\phi)\,[J_n(K_1 r)]$$

$$H_{\phi_1} = -j\frac{\omega\varepsilon_1 A_1 D_1 \cos(n\phi)}{K_1^2 r}\left[K_1 r_e\, J_{n-1}(K_1 r) - n\,J_n(K_1 r)\right]$$

$$H_{r_1} = -j\frac{\omega\varepsilon_1 A_1 D_1 \sin(n\phi)}{K_1^2}\left[J_n(K_1 r)\right]$$

Also:

$$H_{\phi_1} = -j \frac{\omega \varepsilon_1 n A_1 D_1 \cos(n\phi)}{K_1^2 r} \left[J_n(K_1 r)\right]\left[\frac{K_1 r}{n} \frac{J_{n-1}(K_1 r)}{J_n(K_1 r)} - 1\right] \qquad (4.7)$$

and:

$$\frac{\partial H_{r_1}}{\partial \phi} = -j \frac{\omega \varepsilon_1 n^2 A_1 D_1 \cos(n\phi)}{K_1^2 r} \left[J_n(K_1 r)\right] \qquad (4.8)$$

Combining equations (4.7) and(4.8) gives:

$$H_{\phi_1} = \frac{1}{n} \frac{\partial H_{r_1}}{\partial \phi} \left[\frac{K_1 r}{n} \frac{J_{n-1}(K_1 r)}{J_n(K_1 r)} - 1\right] \qquad (4.9)$$

defining

$$G \equiv \frac{K_1 r_c}{n} \frac{J_{n-1}(K_1 r_c)}{J_n(K_1 r_c)}$$

$$H_{\phi_1}(r_c) = \frac{1}{n} \frac{\partial H_{r_1}}{\partial \phi} \left[G - 1\right]$$

5. Fields in Region II

To satisfy the boundary condition at the outer cylindricall wall of the cavity, (The E-field vanishes at a perfect conductor) E_z will be set equal to 0 when $r = r_o$. This will determine the coefficient B_2 in terms of A_2. The result of this process is as shown below:

$$E_{z_2} = A_2 D_2 \cos(n\phi)\left[J_n(K_1 r) - \frac{J_n(K_1 r_0)}{N_n(K_1 r_0)} N_n(K_1 r)\right] \qquad (4.10)$$

$$H_{\phi_2} = -j \frac{K_1 A_2 D_2 \cos(n\phi)}{\omega \mu_1}\left[J_{n-1}(K_1 r) - \frac{J_n(K_1 r_0)}{N_n(K_1 r_0)} N_{n-1}(K_1 r) - \frac{n}{K_1 r} J_n(K_1 r) + \frac{n}{K_1 r} \frac{J_n(K_1 r_0)}{N_n(K_1 r_0)} N_n(K_1 r)\right] \qquad (4.11)$$

$$H_{r_2} = -j \frac{n A_2 D_2 \sin(n\phi)}{\omega \mu_1 r}\left[J_n(K_1 r) - \frac{J_n(K_1 r_0)}{N_n(K_1 r_0)} N_n(K_1 r)\right] \qquad (4.12)$$

6. Induced Currents

The principle of continuity of current requires that the net current (time average) entering the tooth structure be zero. At resonance the inductive current in the tooth structure is equal to the capacitive current. The inductive current will be considered to consist of two parts; namely, a radial component (caused by the angular component of magnetic field) and an angular component (caused by the radial component of magnetic field which threads through the teeth). Use will be made of the relationship:

$$\bar{\tau} = \bar{n} \times \bar{H}$$

That is, the magnetic field intensity at the surface of a perfect conductor is equal in magnitude, and is perpendicular to the linear current density flowing on the conductor. Referring to Fig. 9, the radial component of current flowing into the tooth structure per tooth due to $H_{\phi 2}$ is:

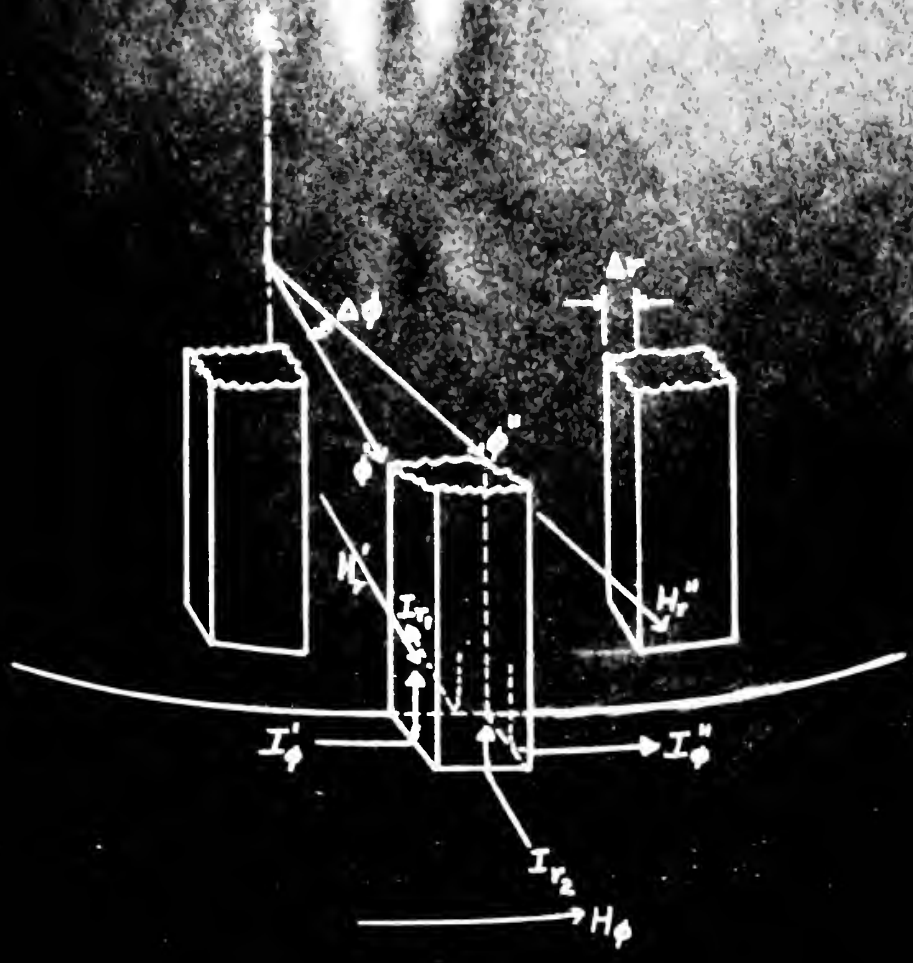

FIG. 9 - TOOTH STRUCTURE SHOWING CURRENTS INDUCED

$$I_{r_2/tooth} = \frac{2\pi r_c}{\alpha} H_{\phi_2}$$

and the current due to $H_{\phi 1}$ is:

$$I_{r_1/tooth} = \frac{2\pi r_c}{\alpha} H_{\phi_1}$$

Also referring to Fig. 9, the angular component of current flowing into the tooth structure per tooth due to H_r' is:

$$I'_{\phi/tooth} = M \Delta r H_r'$$

The current at the other side of the tooth due to H_r'' is:

$$I''_{\phi/tooth} = M \Delta r H_r''$$

The expression for resonant wavelength may be derived under two different assumptions. (a) The end spaces extend over the interaction space and completely enclose the interaction space. Under this assumption, the fields as derived for region I apply. (b) The end spaces do not extend over the interaction space and the magnetic field in the interaction space is essentially radial. Under this assumption $H_{\phi 1}$ is zero. The practical case lies between these two, and hence the true result will lie between the expressions derived

below:

7. Matching Fields at the Tooth Structure

Since the radial component of magnetic field threads through the tooth structure, it is continuous across the boundary. Hence:

$$H_{r_1}(r_t) = H_{r_2}(r_t) \equiv H_r$$

and

$$\frac{\partial H_{r_1}(r_t)}{\partial \phi} = \frac{\partial H_{r_2}(r_t)}{\partial \phi} \equiv \frac{\partial H_r}{\partial \phi}$$

also

$$E_{z_1}(r_t) = E_{z_2}(r_t) \equiv E_z$$

8. Derivation of Wavelength Equations

Under assumption (a), the total inductive current per tooth is:

$$I_{i/tooth} = I_{r_2} - I_{r_1} + I'_\phi - I''_\phi = \frac{2\pi r_t}{\alpha}(H_{\phi_2} - H_{\phi_1}) + M\Delta r(H'_r - H''_r)$$

$$I_{i/tooth} = \frac{2\pi r_t}{\alpha}(H_{\phi_2} - H_{\phi_1}) - M\Delta r \frac{\partial H_r}{\partial \phi}\Delta\phi$$

but

$$\Delta\phi = \frac{2\pi}{\alpha}$$

Hence:

$$I_{i/tooth} = \frac{2\pi r_t}{\alpha}\left[H_{\phi_2} - \left(\frac{G-1}{n} - \frac{M\Delta r}{r_t}\right)\frac{\partial H_r}{\partial \phi}\right] \qquad (4.13)$$

If V is the potential between teeth and $_j$wC is the admittance between teeth, the capacitive current per tooth is given by:

$$I_{c/tooth} = j\omega C V \qquad (4.14)$$

The voltage between teeth is the line integral of the electric field from one plate to the other plate at the radius of the tooth structure. Since E_z does not vary in the z direction, we have:

$$V = E_z d \qquad (4.15)$$

As stated before, at resonance:

$$I_{c/tooth} = I_{i/tooth}$$

from equations (4.13), (4.14), (4.15)

$$E_z = \frac{I_i}{j\omega C d} = \frac{2\pi r_t}{j\omega \alpha C d}\left[H_{\phi_2} - \left(\frac{G-1}{n} + \frac{M\Delta r}{r_t}\right)\frac{\partial H_r}{\partial \phi}\right] \qquad (4.16)$$

Substituting the appropriate quantities from (4.10), (4.11), and (4.12), when they are evaluated ar $r = r_t$

$$A_2 D_2 \cos(n\phi)\left[J_n(K,r_t) - \frac{J_n(K,r_0)}{N_n(K,r_0)} N_n(K,r_t)\right] =$$

$$= \frac{2\pi r_t A_2 D_2 \cos(n\phi)}{\omega \alpha C d}\left\{-\sqrt{\frac{\varepsilon_1}{\mu_1}}\left[J_{n-1}(K,r_t) - \frac{J_n(K,r_0)}{N_n(K,r_0)} N_{n-1}(K,r_t)\right]\right.$$

$$\left. + \left[J_n(K,r_t) - \frac{J_n(K,r_0)}{N_n(K,r_0)} N_n(K,r_t)\right]\left[\sqrt{\frac{\varepsilon_1}{\mu_1}}\frac{n}{K r_t} + \frac{n^2 M\Delta r}{\omega \mu_1 r^2} + \sqrt{\frac{\varepsilon_1}{\mu_1}}\frac{n}{K r_t}(G-1)\right]\right\}$$

Simplifying the above equation gives the wavelength equation:

$$(n\lambda)^2 = \frac{2\pi \alpha C d}{\varepsilon_1\left(\frac{M\Delta r}{r_t} + \frac{G}{n}\right)}\left\{\frac{\left[J_{n-1}(K,r_t) - \frac{J_n(K,r_0)}{N_n(K,r_0)} N_{n-1}(K,r_t)\right]}{\left[J_n(K,r_t) - \frac{J_n(K,r_0)}{N_n(K,r_0)} N_n(K,r_t)\right]}\frac{\lambda r_t \varepsilon_1}{\alpha C d} + 1\right\} \qquad (4.17)$$

Under assumption (b), since $H_{\phi_1} = 0$, we may write equation (4.16) as:

$$E_z = \frac{2\pi r_t}{j\omega \alpha C d}\left[H_{\phi_2} - \frac{M\Delta r}{r_t}\frac{\partial H_r}{\partial \phi}\right]$$

In a similar fashion, as shown above, the wavelength equation becomes:

$$(n\lambda)^2 = \frac{2\pi\alpha C d}{\varepsilon_1\left(\frac{M\Delta r}{r_t} + \frac{1}{n}\right)}\left\{1 + \frac{\lambda r_t \varepsilon_1}{\alpha C d}\left[\frac{J_{n-1}(K,r_t) - \frac{J_n(K,r_o)}{N_n(K,r_o)} N_{n-1}(K,r_t)}{J_n(K,r_t) - \frac{J_n(K,r_o)}{N_n(K,r_o)} N_n(K,r_t)}\right]\right\} \qquad (4.18)$$

Hence, it appears that in the practical case, where the interaction space is only partially enclosed, we may use equation (4.17) provided we use an appropriate value for G between 1 and $\frac{K_1 r_t}{n} \frac{J_{n-1}(K_1 r_t)}{J_n(K_1 r_t)}$. Practical values of G have been found to be close to 1.5.

Using the practical case, the equation for the cavity mode (n = 0) simplifies to:

$$\lambda = \frac{\alpha C d}{\varepsilon_1 r_t}\left[\frac{J_o(K,r_t) - \frac{J_o(K,r_o)}{N_o(K,r_o)} N_o(K,r_t)}{J_1(K,r_t) - \frac{J_o(K,r_o)}{N_o(K,r_o)} N_1(K,r_t)}\right] \qquad (4.19)$$

Equation (4.17) and (4.19) are the principal resonance equations for the interdigital magnetron. Both of these equations are transcendental and require special means of solution. Equation (4.19) may be solved by graphical means. In equation (4.17), the term containing the Bessel Functions is usually negligible and may be neglected and considered as a correction term. The equation may be solved neglecting the

correction term. The resulting wavelength may then be used to find the value of the correction term and λ may be corrected accordingly.

An approximation that will be of some interest may be obtained for the resonant wavelength. The assumption will be made that the gap between teeth is equal to the distance between the end of a tooth and the opposite end plate. If the capacitance (C') between teeth is calculated using the formulae for plane parallel plates, and this capacitance is expressed in terms of M, Δr, α, and r_t , the actual capacitance between teeth is given by:

$$C = \xi C'$$

Using these approximations the wavelength equation becomes:

$$n\lambda \cong \frac{\alpha d + 2\pi r_t}{\sqrt{\frac{1 + \frac{1.5 r_t}{M n \Delta r}}{\xi}}}$$

In the first order mode, the denominator of this expression is found to be about 2 for many interdigital magnetrons. Inasmuch as this is true, it is not surprising that the empirical formula observed by Crawford and Hare (1), was observed to check many experimental tubes. This formula is:

$$\lambda = \frac{\alpha d + 2\pi r_t}{2}$$

9. Wavelength Equation Derived by Lucke (10)

Lucke (10) has developed a wavelength equation based on energy concepts. His wavelength equation is given below.

$$\frac{h}{2\pi a^2}\left[\frac{c_e}{\epsilon_1} - \frac{n^2 L}{h^2 A^2}\right] = \frac{1}{A}\left[\frac{J_{n-1}(A)}{J_n(A)} - \frac{Q_{n-1,n}(A,B)}{Q_{n,n}(A,B)}\right] \qquad (4.20)$$

The equivalence of symbols in this equation to the symbols used in the previous derivation is shown below:

$h = d$ $\qquad$ $C_\epsilon = \alpha C$ $\qquad$ $B = K, r_o$

$a = r_t$ $\qquad$ $A = K, r_t$

$L = 2\pi r_t\, d\, M\Delta r$

$$Q_{n-1,n}(A,B) = J_{n-1}(K,r_t)\,N_n(K,r_o) - J_n(K,r_o)\,N_{n-1}(K,r_t)$$

$$Q_{n,n}(A,B) = J_n(K,r_t)\,N_n(K,r_o) - J_n(K,r_o)\,N_n(K,r_t)$$

and

$$\frac{Q_{n-1,n}(A,B)}{Q_{n,n}(A,B)} = \frac{J_{n-1}(K,r_t) - \frac{J_n(K,r_o)}{N_n(K,r_o)}N_{n-1}(K,r_t)}{J_n(K,r_t) - \frac{J_n(K,r_o)}{N_n(K,r_o)}N_n(K,r_t)}$$

If these quantities are substituted into equation (4.20) and the resultant equation is simplified, equation (4.17) again

results.

In addition to the solution of the wavelength equation, Lucke (10) has derived an expression for C for an anode with no phase shifting teeth. This equation, without derivation, is given below:

$$C = \varepsilon_1 \left[(d - 2g)\left(P_1 + \frac{\Delta r}{m}\right) + w\left(P_2 + \frac{\Delta r}{g}\right) \right]$$

$$P_1 = \frac{1}{\pi}\left[\frac{w+m}{m} \log_e \frac{2m+w}{m} + \log_e \frac{w(2m+w)}{m^2} \right]$$

$$P_2 = \frac{4}{\pi} \log_e \csc \frac{\pi g}{2d}$$

where g is the distance between the end of a tooth and the opposite end plate, w is the width of a tooth, and m is the gap between teeth. If the number of phase shifting teeth is small compared to the total number of teeth, this same expression may be used where phase shifting teeth are employed.

Lucke has also derived an expression for the resonant wavelength when the cathode is present. It is the same as equation (4.17) provded G is determined from the equation given below.

$$G = \frac{K_1 r_t}{n} \left[\frac{J_{n-1}(K_1 r_t) - \frac{J_n(K_1 r_c)}{N_n(K_1 r_c)} N_{n-1}(K_1 r_t)}{J_n(K_1 r_t) - \frac{J_n(K_1 r_c)}{N_n(K_1 r_c)} N_n(K_1 r_t)} \right]$$

The quantity r_c is the cathode radius.

10. Analysis of Factors Affecting Tuning in Cavity Mode

The equation for the resonant wavelength in the cavity mode can be rewritten as follows:

$$\frac{\lambda}{2\pi r_t} = \frac{\alpha C d}{2\pi \varepsilon_1 r_t^2}\left[\frac{J_0(K_1 r_t) - \frac{J_0(K_1 r_0)}{N_0(K_1 r_0)} N_0(K_1 r_t)}{J_1(K_1 r_t) - \frac{J_0(K_1 r_0)}{N_0(K_1 r_0)} N_1(K_1 r_t)}\right] . \qquad (4.20)$$

If we assume r_t is fixed and that the change in d is negligible, and defining quantities as shown below, we may write the equation in a simpler form.

$$F \equiv \left[\frac{J_0(K_1 r_t) - \frac{J_0(K_1 r_0)}{N_0(K_1 r_0)} N_0(K_1 r_t)}{J_1(K_1 r_t) - \frac{J_0(K_1 r_0)}{N_0(K_1 r_0)} N_1(K_1 r_t)}\right]$$

$$T \equiv \frac{\alpha C d}{2\pi \varepsilon_1 r_t^2}$$

$$\frac{\lambda}{2\pi r_t} = \frac{1}{K_1 r_t} = TF \qquad (4.21)$$

If we consider the variables in this equation to be $1/K_1 r_t$ and F, we have a series of straight lines passing through the origin. The slope of these lines is inversely proportinal to C. Now, if we plot F as a function of $1/K_1 r_t$ for various values of the ratio r_o/r_t, we have a family of curves. The intersection of the straight line determined by

C with the curve determined by r_o/r_t gives us the value of $\frac{1}{K_1 r_t}$. From this value, we may determine λ from:

$$\lambda = \frac{2\pi r_t}{K_1 r_t}$$

A plot of the quantities discussed above is shown in Fig. 10. From this plot certain things may be deduced. If capacitance alone is varied and the outer radius is kept fixed, the wavelength varies as C^p where p lies between 0.484 and 0.424. Here p takes on the larger values for small values of R. If the capacitance is held constant, however, and R is varied, the variation in wavelength cannot be expressed so neatly. However, if we express it in the same fashion as before, we may make some comparisons between capacity tuning and cavity tuning. Taking λ as proportional to R^p, we find that p varies between 0.604 and 0.374. Here p is greatest for small C and small R and is least for large C and large R. Hence, for greatest tuning ranges interdigital magnetrons should be designed so that the parameters fall in the lower left hand region of the chart. However, this consideration is not particularly critical, and magnetrons may be designed from any point on the chart without too great a loss in tuning range.

11. External Q Calculations

The external Q of a cavity is defined as follows:

$$Q_e = \omega \frac{\text{Energy stored in cavity}}{\text{Average power output}} \qquad (4.22)$$

FIG. 10

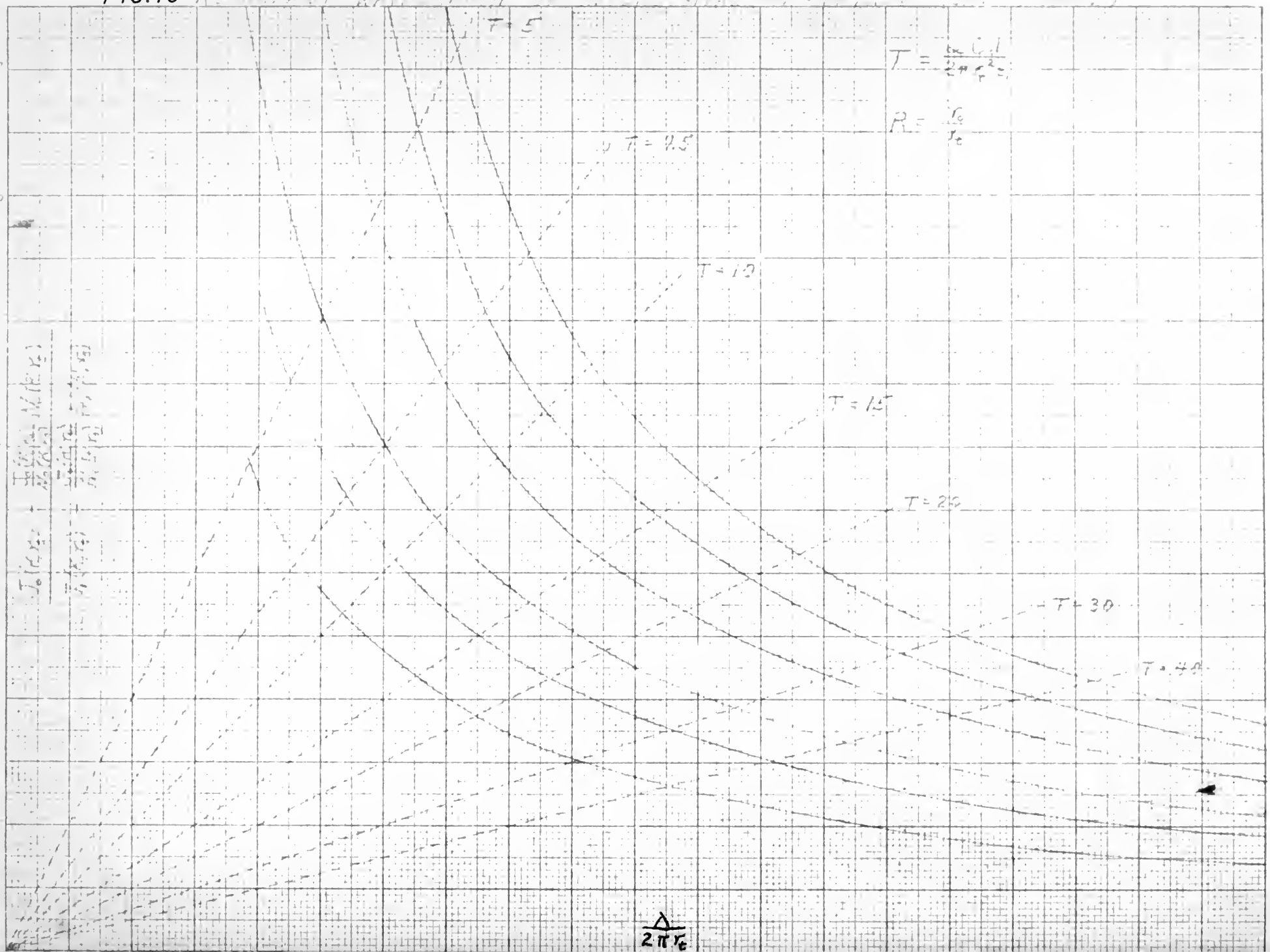
T = 5
T = 11.5
T = 17
T = 25
T = 30
T = 40
$T = \frac{t_w C_f l}{2\pi r_c^2 \gamma}$
$R = \frac{r_o}{r_c}$
$\frac{\Delta}{2\pi r_c}$

In order to simplify the calculations, it will be assumed that the power is coupled out by a loop.

The total loop voltage is equal to the difference between the voltage induced by the changing flux through the loop, and the IZ drop in the loop. Assuming that only the Hø field passes through the loop and that the loop is a pure inductance, we have the rms loop voltage given by:

$$V_\ell = S\mu_1 \left| \frac{\partial H_{\phi_0}}{\partial t} \right| - j\omega I_\ell L$$

But

$$I_\ell = \frac{V_\ell}{Z_0}$$

and

$$\left| \frac{\partial H_{\phi_0}}{\partial t} \right| = \omega \left| H_{\phi_0} \right|$$

Therefore,

$$\left| V_\ell \right|^2 = \frac{S^2 \mu_1^2 \omega^2 \left| H_{\phi_0} \right|^2}{1 + \frac{\omega^2 L^2}{Z_0^2}}$$

The power delivered to the output line is then

$$P_o = \frac{|V_z|^2}{Z_o} = \frac{s^2 \mu_1^2 \omega^2 |H_{\phi_o}|^2}{Z_o + \frac{\omega^2 L^2}{Z_o}} \qquad (4.23)$$

Since the electric and magnetic fields are in time quadrature, the energy stored in the cavity may be determined from the electric field when it is a maximum. Thus, the electric field energy stored in the cavity per radian is

$$U_{\varepsilon/\text{radian}} = \int_{r_t}^{r_o}\int_{0}^{d} \frac{\varepsilon_1 |E_z|^2}{2} r\, dr\, dz = \varepsilon_1 d \int_{r_t}^{r_o} \frac{r |E_z|^2}{2} dr$$

The peak electric field energy stored in the tooth structure per radian is

$$U_{t/\text{radian}} = \frac{\alpha C}{2\pi} \frac{|E_z d|^2}{2}$$

Integrating the sum of these two functions around the cavity, the following expression for the total energy stored in the cavity is obtained.

$$U_T = \frac{a d A^2 D^2}{2} \left\{ \pi \varepsilon_1 \int_{r_t}^{r_o} r \left[J_n(K,r) - \frac{J_n(K,r_o)}{N_n(K,r_o)} N_n(K,r) \right]^2 dr \right.$$

$$\left. + \frac{\alpha C d}{2} \left[J_n(K,r_t) - \frac{J_n(K,r_o)}{N_n(K,r_o)} N_n(K,r_t) \right] \right\} \qquad (4.24)$$

In this expression a=2 when n=0 and a=1 when n>0.

It may be shown that the value of the term under the integral sign containing the Bessel functions is fairly constant as r is varied. Making this approximation we have for the term under the integral sign.

$$\pi \varepsilon_1 \left\{ r_t \left[J_n(K_1 r_t) - \frac{J_n(K_1 r_0)}{N_n(K_1 r_0)} N_n(K_1 r_t) \right]^2 \left(\frac{r_0 - r_t}{2} \right) \right\}$$

Substituting this expression into equation (4.24) and combining equations (4.22), (4.23) and (4.24) we obtain the following expression for Q_e

$$Q_e = \frac{\omega a d \left[Z_0 + \frac{\omega^2 L^2}{Z_0} \right] \left[\pi \varepsilon_1 r_t (r_0 - r_t) + \alpha C d \right] \left[J_n(K_1 r_t) - \frac{J_n(K_1 r_0)}{N_n(K_1 r_0)} N_n(K_1 r_t) \right]^2}{2 S^2 K_1^2 \cos^2(n \phi_t) \left[J_{n-1}(K_1 r_0) - \frac{J_n(K_1 r_0)}{N_n(K_1 r_0)} N_{n-1}(K_1 r_0) \right]^2}$$

ϕ is the angle between the current maximum and the loop. Ordinarily ϕ will be equal to either 0 or $\frac{\pi}{2}$. With mode favoring or suppressing devices such as phase shifting teeth, however, ϕ is arbitrarily fixed.

12. Experimental Results

The formulae for resonant wavelength have been checked by Hull (9) and Lucke (10). The results of these measurements have checked very closely with calculated values. In most cases, the error has been less than 3%. Hull has also checked the formula for external Q and has found good agreement be-

tween calculated and measured values.

CHAPTER V

OPERATION IN THE ZERO ORDER MODE

1. Introduction

The results of the work of some of the early experimenters has been discussed in a preceding chapter. It will be noted that all of these earlier interdigital magnetrons operated either in the first order mode or with low power output and low efficiency in the zero order mode. The power output and efficiency obtained in the first order mode was also low. Since electronic efficiency and hence, overall efficiency should be highest in the cavity mode, where a simple pi-mode field configuation is presented to the cathode, it was felt desirable to determine why the interdigital magnetrons would not operate in the cavity mode at high values of current. The reason for poor operation in the cavity mode was determined and a remedy devised by Mr. J. F. Hull of the Evans Signal Laboratory in 1947, and successful tubes delivering comparatively high power were constructed. The reason for poor operation was determined to be radiation from the cavity in the cavity mode. This phenomena had also been noted by Dench and Barrow in 1940.

The reason for the radiation in the zero order mode and the lack of radiation in the first order mode can be seen from an inspection of Fig. 2 and Fig. 3. In Fig. 2, we see that the electric field vectors in the vicinity of the cathode in the zero order mode are in the same direction everywhere around

the cathode, and hence there is a voltage induced in the cathode which causes currents to flow axially along the cathode. This current flowing through the cathode causes radiation from the cathode leads. Now, if we look at Fig. 4, we see that the electric field vectors are in opposite directions on opposite sides of the cathode in the first order mode. Hence, the net voltage induced in the cathode is zero and the cathode does not radiate energy. This is true, if the system is perfectly symmetrical. The remedy for this difficulty will be discussed in full in a later secion of this chapter.

In addition to the fact that higher power and efficiency can be obtained in the cavity mode, there are other reasons for preferring operation in the cavity mode. Construction of the anode for operation in the first order mode is more complicated due to the necessity for phase-shifting teeth, degenerate mode suppressing devices or other means of encouraging operation in the first order mode. Also, the possible tuning range is greatest in the cavity mode. Although the variation of wavelength in both modes is approximately proportional to $\sqrt{C}$, the tuning range with varying cavity dimensions is quite different for the two modes. In the first order mode, the wavelength is relatively independent of the cavity dimensions. In the cavity mode, however, the wavelength varies approximately as $\sqrt{r_o/r_t}$. This difference is shown graphically in Fig. 11 and Fig. 12.

TYPICAL TUNING CURVE OF ZERO
FIG. 12

Since these factors favor operation in the zero order mode, all of the discussion in the remainder of this chapter will assume operation in the cavity mode unless otherwise stated.

2. Cathode Decoupling

As we have mentioned before, the reason for poor operation in the cavity mode is radiation from the cathode leads. The effect of the radiation is to introduce losses into the circuit and hence to reduce the unloaded Q of the circuit. Our problem, then, is one of reducing the radiation from the cathode. In Fig. 13(a), we see a cutaway view of an interdigital magnetron, and in Fig. 13(b) is shown an equivalent circuit for the interdigital magnetron. In this circuit, C_t is the excess capacitance of the tooth structure, or in the symbols used in the preceding chapter, $\propto C$. G represents the losses present in the cavity and output. L is the fictional lumped inductance required to resonate with C_t at the operating frequency. C_2 is the shunt capacitance caused by the discontinuities at point A. Likewise, C_1 is the shunt capacitance caused by the discontinuities at point B. Z_2 is the impedance presented by the cathode line at point A. Likewise, Z_1 is the impedance presented by the tuner mechanism at point B. Equivalent circuits of this type have been checked experimentally by Hull (8) and Welch (16). If we replace the parallel combination of C_1 and Z_1 by Z_1' and assume that $Z_1' = -jX_1'$ and let $Z_2 = R_2 \pm jX_2$ we find the power dissipated in R_2 to be

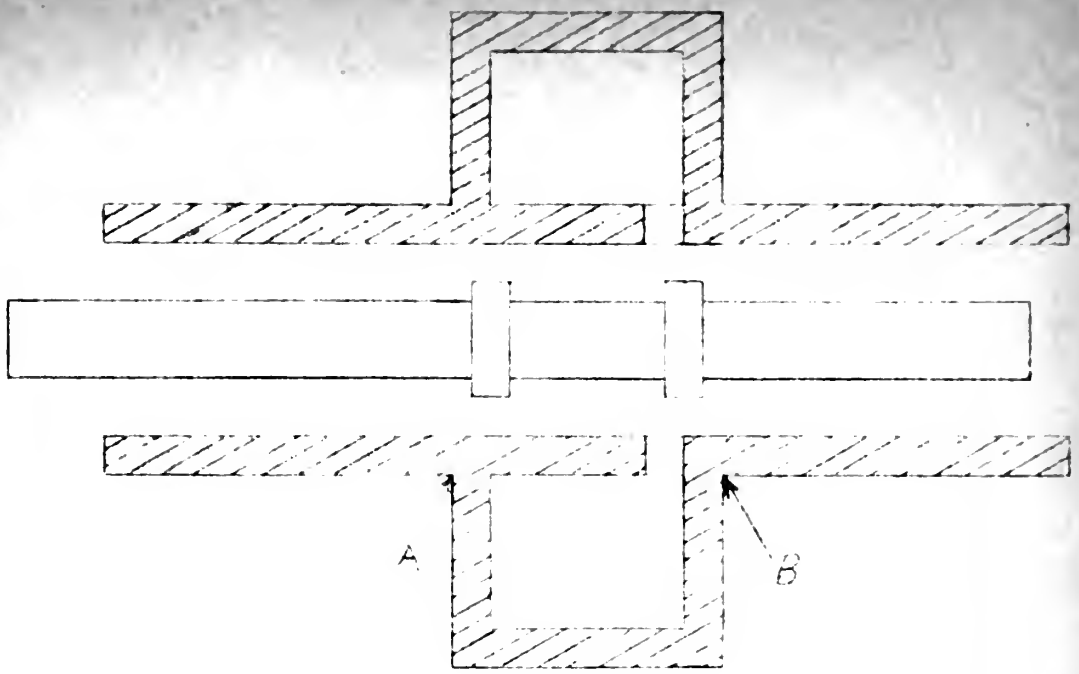

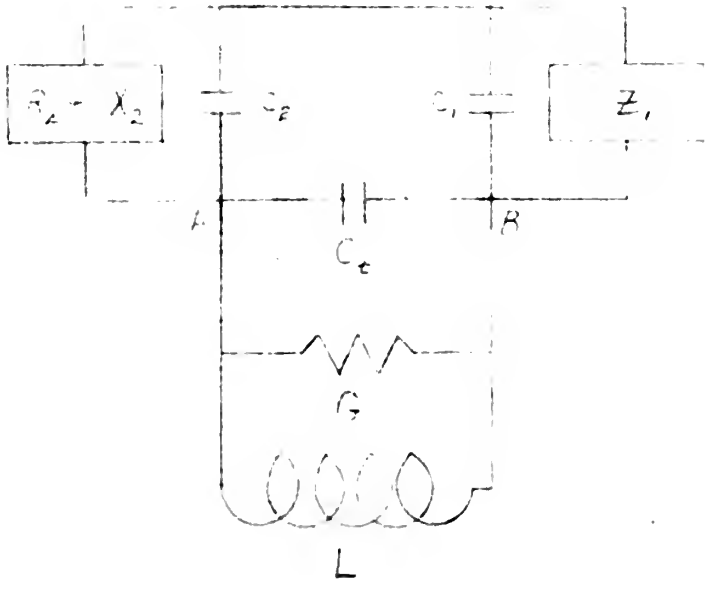

Fig 13 - CUTAWAY VIEW OF INTERDIGITAL MAGNETRON AND ITS EQUIVALENT CIRCUIT

$$P = \frac{E^2 R_2}{R^2(1+\omega C_2 X_1')^2 + [X_2(1+\omega C_2 X_1') - X_1']^2} \qquad (5.1)$$

It can be seen that if $X_2 = \infty$, the power coupled out the cathode line is a minimum. If Z_1 is much greater than $1/\omega C_1$, the expression for the power dissipated in R_2 becomes,

$$P = \frac{E^2 R_2}{R^2\left(1+\frac{C_2}{C_1}\right)^2 + \left[X_2\left(1+\frac{C_2}{C_1}\right) - \frac{1}{\omega C_1}\right]^2}$$

If X_2 is a very large capacitive reactance, C_1 should be made small for minimum power into R_2. This also demands that C_2 be made small in order to prevent unbalancing the cathode.

The power in the load can be obtained from

$$P_o = E^2 G$$

if G is determined from the external Q determined when the cathode is absent. From the ratio of these two powers, we may obtain the percentage of output power lost in the cathode circuit.

In order to obtain the required high value of reactance, it is necessary to place a short circuit a quarter wavelength down the cathode line from point A. Since there is a DC

potential between the cathode and the anode, this cannot be done. Hence, a choke and bypass combination or "non-contacting short" must be used. The next section will provide criteria for the design and placement of an effective "short".

If we place a choke and bypass combination which has an impedance Z_3 at a distance l down the line from point A, we have,

$$Z_2 = Z_0 \left[\frac{Z_3 \cos\beta l + j Z_0 \sin\beta l}{Z_0 \cos\beta l + j Z_3 \sin\beta l} \right]$$

where Z_0 is the characteristic impedance of the cathode line. In order to satisfy the requirement that $X_2 = \infty$ or $B_2 = 0$, the following equation must be satisfied.

$$B_3 Y_0 (\cos^2\beta l - \sin^2\beta l) + (B_3^2 - Y_0^2 + G_3^2)(\sin\beta l \cos\beta l) = 0$$

If the choke and bypass combination is designed so that G_3 may be neglected, the above equation reduces to

$$\tan 2\beta l \cong - \frac{2 B_3 Y_0}{B_3^2 - Y_0^2} \qquad (5.2)$$

From this equation, the length l may be determined and the choke and bypass may be properly placed.

Two designs of chokes will be shown and expressions will be derived for the impedance seen looking into the right hand

end of the choke. This corresponds to the quantity Z_3 as used above.

In Fig. 14 is shown a choke which is shorted to the cathode but does not touch the pole piece. If l_1 is made equal to $\lambda/4$, the impedance presented by the coaxial line of characteristic impedance Z_o' formed by the choke and cathode pole piece is

$$Z_a = \frac{Z_o'^2}{Z_o}$$

Now, if we consider the coaxial line made up of the cathode and choke of length l_2 and characteristic impedance Z_o'', which is shorted at one end, we find the impedance presented at the other end to be

$$Z_b = j Z_o'' \tan \beta l_2$$

and hence Z_3, which is the sum of Z_a and Z_b, is

$$Z_3 = \frac{Z_o'^2}{Z_o} + j Z_o'' \tan \beta l_2$$

If the dimensions of the cathode, choke, and pole piece are made such that

$$Z_o \gg Z_o'' \gg Z_o'$$

FIG.

and if l_2 is made close to a quarter wavelength

$$\frac{Z_o'^2}{Z_o} << Z_o'' \tan\beta l_2$$

and

$$Z_3 \cong j Z_o'' \tan\beta l_2$$

or

$$Y_3 \cong j B_3 \cong -j Y_o'' \cot\beta l_2$$

Thus, using this type of choke, we can find the length l needed to satisfy the equation,

$$\tan 2\beta l \cong \frac{2 Y_o'' Y_o \cot\beta l_2}{Y_o''^2 \cot^2\beta l_2 - Y_o^2} \qquad (5.3)$$

Another type of choke and bypass combination can be made which is shorted to the cathode pole piece but does not touch the cathode. This is shown in Fig. 15. Note should be taken that some of the quantities have been given new significance in the drawing. If the quantities are defined as shown in Fig. 15 and the same restrictions are applied to the quantities as were applied to the same quantities in the derivation shown above, the same expression determining l may be used, namely;

$$\tan 2\beta l \cong \frac{2 Y_o'' Y_o \cot \beta l_2}{Y_o''^2 \cot^2 \beta l_2 - Y_o^2}$$

One of the drawbacks to the use of chokes designed as shown above is that the bandwidth over which they are effective is somewhat limited. If the full range of tuning possible in the cavity mode is to be realized, chokes of broader bandwidth must be used or the possibilities of tunable chokes must be explored.

As previously shown, we may reduce the power dissipated in the cathode lead by decreasing C_1 and C_2. This may be done by cutting recesses in each end surface so that the teeth from the opposite and surface may pass through. This has been done by Hull and the improvement was noticeable.

Fig. 16 shows an interdigital magnetron constructed at the University of Michigan. In this photograph are shown the important parts used in the magnetron. In addition there is shown the completely assembled tube. The chokes used in this model are of the type shown in Fig. 15.

3. Interaction Space Design

Using the work of Slater and Allis, the Electron Tube Laboratory of the University of Michigan has set up an analysis of factors affecting the design of the interaction space of interdigital magnetrons. The problems that exist here are of the same type as those encountered in the design

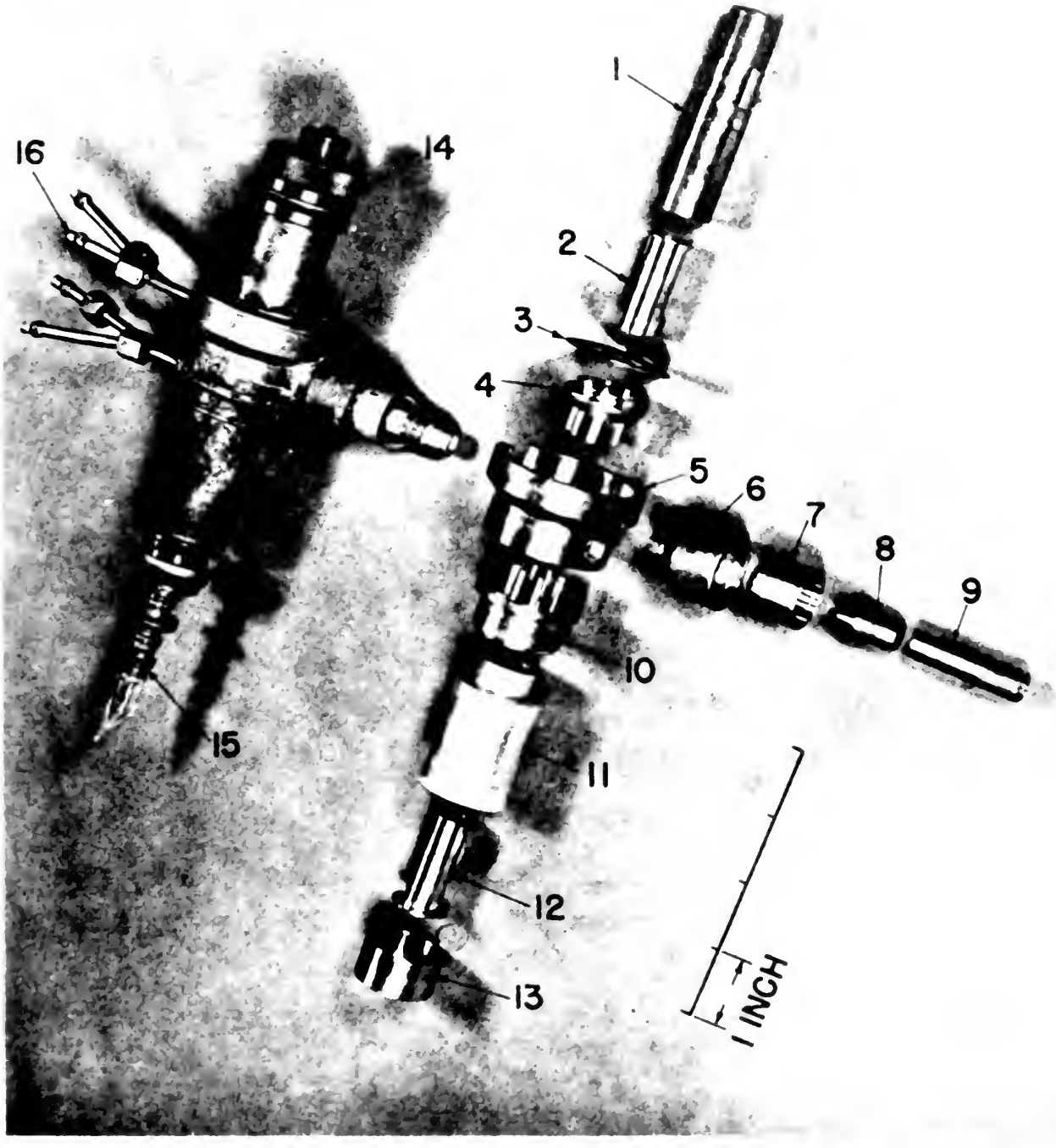

Fig. 16 Interdigital Magnetron Constructed at the University of Michigan

1. Tuner screw
2. Tuner choke
3. Diaphragm
4. Diaphragm anode
5. Cavity
6. Outside taper
7. Outside Kovar
8. Inside taper
9. Inside Kovar
10. Cavity anode
11. Cathode pole piece
12. Cathode choke
13. Kovar sleeve
14. Tuner pole piece assembly
15. Cathode assembly
16. Water cooling tubes

of multicavity magnetrons. Certain points, however, are deserving of special consideration.

Certain design parameters have been set up for scaling of magnetrons which may be used in the design of magnetrons. These design parameters which depend on the dimensions of the interaction space and the resonant wavelength are defined as follows:

$$E_o = \frac{m}{2e}\left(\frac{2\pi c}{n\lambda}\right)^2 r_t^2 \qquad \text{volts} \qquad (5.4)$$

$$B_o = \frac{2m}{e}\left(\frac{2\pi c}{n\lambda}\right)\frac{1}{1-\left(\frac{r_c}{r_t}\right)^2} \qquad \text{webers/meter} \qquad (5.5)$$

$$I_o = \frac{2\pi a_1}{\left[1-\left(\frac{r_c}{r_t}\right)^2\right]^2\left[\frac{r_t}{r_c}+1\right]}\frac{m}{e}\left(\frac{2\pi c}{n\lambda}\right)^3 r_t^2 \varepsilon_o L \qquad \text{amperes} \qquad (5.6)$$

where: n = a mode number ($\alpha/2$ for zero order mode, $\alpha/2 \pm 1$ for first order mode)

a_1 = approximately 1 in range of r_t/r_c between 1.3 and 3.5

L = length of emitting surface

In terms of these quantities, the Hartree voltage (i.e. the minimum voltage that will cause oscillations to start at a given value of magnetic field) for the start of oscillations at a given magnetic field is,

$$E = E_o \left(\frac{2B}{B_o} - 1 \right) \qquad (5.7)$$

and the maximum electronic efficiency is given by,

$$\eta_e = 1 - \frac{E_o}{E} \qquad (5.8)$$

This indicates, that for high electronic efficiency E_o/E must be small. That is, for example, it must be less than 1/5 for electronic efficiency higher that 80%.

It has been found experimentally that the current at which magentrons stop oscillating is given by the following approximate relationship;

$$\frac{I}{I_o} = \frac{1}{2} \left(\frac{E}{E_o} \right)^{3/2}$$

It has also been found that operation at small values of I/I_o, say less than 0.1, tends to be inefficient.

Thus we have at our disposal a number of interrelated variables such as E, B, P_o, C, r_t, r_c, r_o, α, L, and λ. However, we have placed a number of restrictions on these variables in the equations above and in the equations in the preceding chapter. Usually a tube is designed for a specific

frequency, so that λ is fixed. The size of the cathode is fairly well fixed by the power output, current, back bombardment power and the available emission density. A knowledge of these cathode factors is a study in itself and will not be undertaken here.

In order to dissipate large amounts of power in the anode, the fingers should be made short and thick, especially at the base of the fingers. Of course the thickness of the fingers affects their capacitance and it is quite likely that a compromise may have to be reached in regard to the thickness of the fingers. In order to get greater variation in capacitance and hence a greater tuning range, tapered teeth with a tab on the end may be used. The heat dissipating qualities are not greatly reduced by such a construction. Reference (16) states that it is believed that no great difficulty should be encountered in dissipating a kilowatt of anode power.

The circuit efficiency in the zero order mode is likely to be low since the unloaded Q is decreased by the effect of the cathode line. In order to achieve high circuit efficiency, low values of Q_l must be used, since,

$$\eta_c = 1 - \frac{Q_c}{Q_u}$$

A typical value of unloaded Q is less than 500, so that for circuit efficiency greater than 80%, Q_l's less than 100 must be used. It appears feasible, therefore, that if a circuit

efficiency of 80% and an electronic efficiency of 80% can be obtained, overall efficiencies of the order of 64% can be obtained. This has been demonstrated experimentally, since overall efficiencies of 70% have been obtained.

Another problem of concern is mode jump current. Experimental evidence seems to indicate that in order to increase mode jump current, we should either increase Q_1 or increase mode separation. The first of these tends to conflict with conditions for high efficiency. The mode separation is increased by increasing C and increasing r_o/r_t.

The voltage separation of the zero and first order modes may be determined from the equations for the Hartree voltage, Eq. (5.7), for the two modes. Thus we find the ratio of the Hartree voltages for these modes to be,

$$\frac{E^{(1)}}{E^{(0)}} = \frac{E_o^{(1)} B_o^{(0)}}{E_o^{(0)} B_o^{(1)}} \frac{2B - B_o^{(1)}}{2B - B_o^{(0)}} \qquad (5.9)$$

If E/E_o is large, as it should be for high efficiency, Eq.(5.9) becomes, approximately,

$$\frac{E^{(1)}}{E^{(0)}} \cong \frac{\alpha}{\alpha + 2} \frac{\lambda_o^{(0)}}{\lambda_o^{(1)}}$$

In order for this ratio to be large for good voltage separation, α should be large. A large number of teeth is indicative of high excess capacitance. High capacitance helps to

give high efficiency and large mode separation. This gives a hint of the direction to be taken on future designs of interdigital magnetrons.

4. Tube Performance

Hull has built interdigital magnetrons which operated well in the zero order mode. A pulsed power output of 1500 watts (peak) at 60 to 80% efficiency with 5% duty cycle was obtained. Five hundred watts of CW power was obtained at efficiencies between 65 and 75%. The limiting factor on this tube was the power loss in the output seal. The tubes built at the University of Michigan have not been too successful due to construction difficulties which are not inherent in the interdigital magnetron. However, they have produced tubes which gave 500 wats of CW power at 70% efficiency.

5. New Applications

In the last two years considerable work has been done, principally by the University of Michigan, on new applications and uses for interdigital magnetrons operating in the zero mode. Some of these developments will be discussed qualitatively here. For a more complete description and discussion, see the University of Michigan Technical Reports(15-21).

One of the new developments is an FM magnetron of the interdigital type. Referring to Fig. 13, we see an equivalent circuit for the interdigital magnetron. The resonant frequency of this circuit is varied by the impedence presented by the cathode line. If we go down the cathode line and place

a variable reactance across the line, we can vary the impedance which the cathode line presents to the magnetron and hence, vary the resonant frequency of the circuit. This has been done by constructing a second magnetron on the cathode some distance down the cathode line. If the voltage on this magnetron is varied, its shunt reactance across the cathode line varies and thus varies the frequency of the first magnetron. Tubes of this type have been built, but operation has not been successful due to leakage of power out the cathode line.

Since, as far as the frequency of oscillation is concerned, the finger structure is just a simple capacitance shunting a resonant circuit, other configurations of interdigital magnetrons seem possible. One possible variation is to make the resonant cavity a section of coaxial line, shunted at one end by the capacitance of the teeth and shorted at the other. Work is being done on this type of structure at the University of Michigan, but little is known concerning its state of progress.

Another development in progress at the University of Michigan is a double anode interdigital magnetron. In this tube, two interdigital structures are placed inside of a single rectangular cavity. The two structures are separated by an integral number of half wavelengths so that they operate in phase. Preliminary tests seem to indicate that the two magnetrons lock in on the same frequency and that the power output is essentially doubled. This same basic idea

may be carried over to include a number of interdigital magnetrons operating in cascade to obtain very high power operation.

CHAPTER VI

CONCLUSIONS AND RECOMMENDATIONS

From work which has been presented in the preceding chapters, it is clear that operation of CW interdigital magnetrons at high power levels is possible. It appears that insufficient work has been done to date to determine what the ultimate limit of power might be. It seems feasible, however, that with fixed frequency tubes, CW power of one or two kilowatts should be possible with single tubes. The recent work with multi-anode interdigital magnetrons seems to offer hope of attaining even higher powers. However, there are some advantages and disadvantages of the interdigital magnetron which should be mentioned.

One of the chief advantages of the interdigital magnetrons is its inherently large mode separation. This, as we have said, is due to the fact that only one resonant system is used instead of the N-mutually coupled resonators of the multicavity magnetron. Another advantage is the possibility of wide tuning ranges. If certain problems are solved, it appears that tuning ranges of 2 or 2.5 to 1 may be possible. The wide mode separation should help to eliminate any possibilities of mode crossovers and thus eliminate some of the problems which have been encountered in multicavity magnetrons. Also, since there is no complicated tuner, troublesome tuner resonances should be practically eliminated. Another minor advantage is that some of the analytical solutions involved in the study of interdigital magnetrons

are more simple than those encountered in multicavity magnetrons. This fact could lead to use of the interdigital magnetron as a tool in gaining a better understanding of the behavior of magnetrons.

Some of the disadvantages and problems encountered with the interdigital magnetron are serious and solutions to these problems must be obtained before the full possibilities of the tubes can be realized. One of the major problems is that of eliminating the cathode radiation over a wide range of frequencies. If this is not done, the inherent mode separation of the interdigital magnetron is utterly meaningless. This demands that either the choke and bypass be made broadband or that the choke and bypass be made tunable. Another problem which must be solved before a truly wide range tunable tube can be built is that of tuning the cavity efficiently. Since, ordinarily the cavity is vacuum tight, it is almost impossible to vary its outer radius. An external cavity tube brings other problems into the picture. A possible solution to this problem will be discussed.

One possible solution to the problem of cathode leakage which occurs to this author is to use an external choke. This choke would be placed outside of the vacuum envelope so that the position of the choke along the cathode line could be varied as the frequency is varied. The vacuum seal should be made very close to point A. A good low loss ceramic bushing having a low dielectric constant could possibly be used for this seal. However, as the frequency is varied, the

length of the choke, in wavelengths, varies. This would cause us to violate some of the assumptions made in the discussion on choke design in the preceding chapter. It is believed that a system similar to that shown in Fig. 17 might help to solve this difficulty. The choke would be designed and placed as shown for the highest frequency to be used. The same design criteria as developed before would apply if the dielectric constant of the ceramic bushing is close to unity. The length βl would now be

$$\beta l = \beta l_3 + \beta_b l_b$$

By proper choice of values, the distance from the choke short to the resonator ($\beta l + \beta l_2$) can be made approximately $\lambda/4$ at this frequency. Now, if the dielectric constant of the ceramic lining is made equal to 4, we find that the position of the choke is approximately correct and the length is approximately correct for a frequency equal to one half of the original frequency. This is true because the lengths involved are electrically the same. Since

$$\beta l = \omega l \sqrt{\mu_1 \epsilon_1}$$

we can easily show this. The length of the choke electrically is unchanged for frequency has been halved and the dielectric constant has been multiplied by four, thus leaving β constant. The position is unchanged for in this region β has been halved

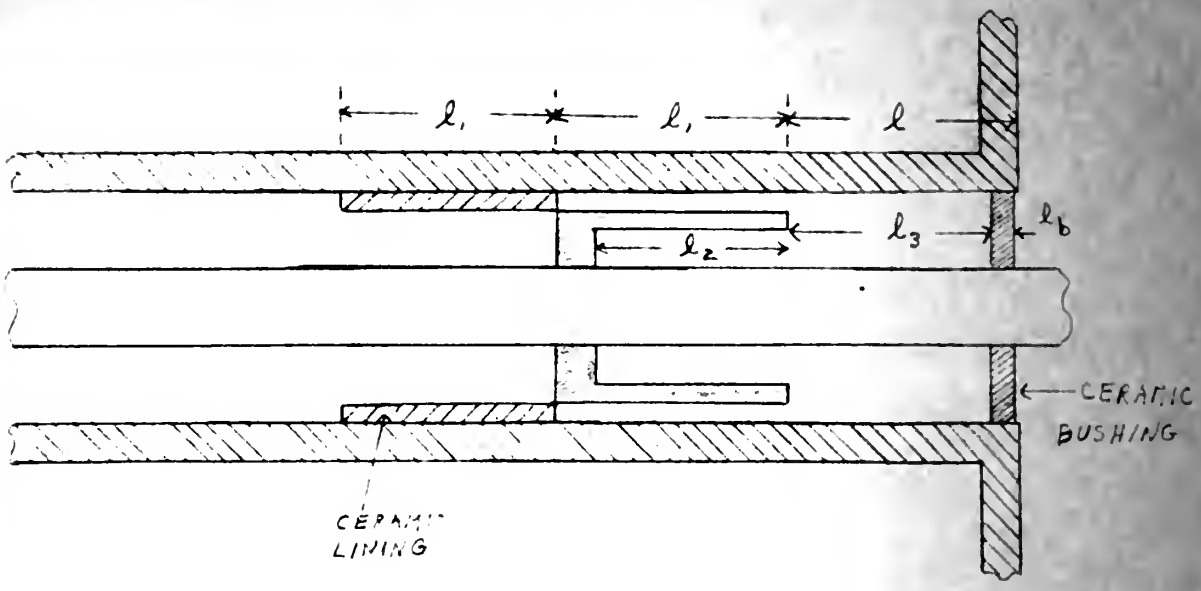

FIG. 17 - SUGGESTED DESIGN OF TUNABLE CHOKE

and l has been approximately doubled, leaving their product a constant.

It appears that the best solution to a wide range tunable tube is to construct a tube with an external cavity so that both the tooth capacitance and cavity radius can be varied. It appears that this might be done in a fashion similar to that used by Sylvania in their external cavity tube. It is suggested that the possibilities of using a low loss ceramic as the vacuum envelope for such a tube should be investigated. The cavity could be made in two halves which join together in a plane containing the axis of the tube. It is possible to do this since the current in theend surfaces is all in a radial direction. The two halves could be clamped onto fins on the tube. Of course this joint would have to be very good as currents would have to flow from the tube to the cavity. This type of construction would not only help increase the tuning range, but would also aid in the analysis and understanding of the multi-anode magnetrons. Investigation of the field in the operating multi-anode tube could be investigated to determine its modes of operation.

Another problem which should be investigated is that of output design. A possible suggestion here is the investigation of waveguide outputs. If an external cavity tube is built, such a waveguide output would not need to be vacuum tight and hence, no output window would be necessary. Probably an iris or simple taper would be sufficient to give

broadband matching. This output section could be made as long as necessary since it is really external to the tube. The waveguide would be joined to the outer cylindrical wall of the cavity with its long dimension parallel to the end surfaces. Such a design, if proved workable, could provide an output system capable of handling large powers over a wide range of frequencies. Such a system is extremely difficult if not impossible to build where the output system must also be vacuum tight.

It is believed that the interdigital magnetron offers some distinct possibilities as a high power source of CW microwave energy having a wide range of frequencies. The possibilities of their use as pulsed oscillators does not seem so good. The CW power delivered by these tubes is comparable to that obtainable with multicavity magnetrons while their possible tuning range is much greater. In view of the fact that so little work has been done on interdigital magnetrons as compared to the enormous amount of work which has been done on multicavity magnetrons, it is felt that a great deal more effort should be spent on the interdigital magnetron. It is hoped that, with such additional effort directed toward the solution of the above problems, we may obtain interdigital magnetrons which will be extremely useful in countermeasures equipments.

BIBLIOGRAPHY

1. Crawford, F. H. and Hare, M. D. Tunable Squirrel Cage Magnetron - the Donutron. Proceedings of the Institute of Radio Engineers. 35:361-369, April 1947.

2. Dench, E. C. Investigation of a Resonant Cavity Magnetron. A thesis for the Degree of Master of Science from the Massachusetts Institute of Technology. 1940.

3. Fisk, J. B., Hagstrum, H. D. and Hartman, P. L. The Magnetron as a Generator of Centimeter Waves. The Bell System Technical Journal. 25-2:167-349, April 1946.

4. Gutton, H. and Berline, S. Research on the Magnetrons; SFR Ultra-shortwave Magnetrons. Bulletin of the Electrical Society of France. 12:30-46, 1938.

5. Hare, M.D. and Leonard, Virginia. The Construction of the Donutron, A Tunable Squirrel Cage Magnetron. Radio Research Laboratory Report No. 411-249, October 26,1945.

6. Hull, J. F. Mathematical Treatment of Modes in the Squirrel Cage Interdigital Magnetron. Memorandum for File, Signal Corps Engineering Laboratories, Fort Monmouth, New Jersey, November 21, 1946.

7. Hull, J. F. and Randals, A. W. A High Power Interdigital Magnetron. ESM-15, Engineering Report No. E-1015, Signal Corps Engineering Laboratories, Fort Monmouth, New Jersey, October 29, 1947.

8. Hull, J. F. and Randals, A. W. High Power Interdigital Magnetrons. Proceedings of the Institute of Radio Engineers, 36:1357-1363, November 1948.

9. Hull, J. F. and Greenwald, L. W. Modes in Interdigital Magnetrons. Proceedings of the Institute of Radio Engineers, 37:1258-1263, November 1949.

10. Lucke, W. S. Obstacle-loaded Cylindrical Cavities with Application to the Interdigital Magnetron. Cruft Laboratory Technical Report No. 60, November 1, 1948.

11. Ludi, F. Theory of Transit Time Oscillations. Helvetia Physica Acta. 13-2:77-121, 1940.

12. O'Neill, G. D. Separate Cavity Tunable Magnetrons. Electronic Industry. 5:48-50, June 1946.

13. Ramo, S. and Whinnery, J. R. Fields and Waves in Modern Radio. J. Wiley, New York, 1944.

14. Radiation Laboratory Series No. 6. Microwave Magnetrons. McGraw-Hill, New York, 1948.

15. Welch, H. W., Jr. Space Charge Effects and Frequency Characteristics of CW Magnetrons Relative to the Problem of Frequency Modulation. Electron Tube Laboratory of the University of Michigan,Technical Report No. 1, November 15, 1948.

16. Welch, H. W.,Jr., and Brewer, G. R. Operation of Interdigital Magnetrons in the Zero Order Mode. Electron Tube Laboratory of the University of Michigan, Technical Report No. 2, May 23, 1949.

17. Welch, H. W.,Jr., Black, J. R., Brewer, G. R., and Hok, G. Theoretical Study, Design and Construction of CW Magnetrons for Frequency Modulation. Electron Tube Laboratory of the University of Michigan, Technical Report No. 3, May 27, 1949.

18. Welch, H.W.,Jr., Black, J. R., and Brewer, G. R. Theoretical Study, Design and Construction of CW Magnetrons for Frequency Modulation. Electron Tube Laboratory of the University of Michigan, Interim Report, December 15, 1949.

19. Welch, H. W.,Jr., Black, J. R., Brewer, G. R. and Hok, G. Theoretical Study, Design and Construction of CW Magnetrons for Frequency Modulation. Electron Tube Laboratory of the University of Michigan, Quarterly Report No. 1, April 1950.

20. Welch, H. W., Jr., Black, J. R., Brewer, G. R., Needle, J. S. and Peterson, W., Theoretical Study, Design and Construction of CW Magnetrons for Frequency Modulation. Electron Tube Laboratory of the University of Michigan, Quarterly Report No. 2, June 1950.

21. Welch, H.W. Jr., Black, J. R., Brewer, G. R., Needle, J. S., Peterson W., Batten, H. W. and Ruthberg, S. Theoretical Study, Design and Construction of CW Magnetrons for Frequency Modulation. Electron Tube Laboratory of the University of Michigan, Quarterly Report No. 3.

22. Young, R. T. Jr., Holmboe, L. W., and Waters, W. E. Some Observations on the Back Heating of Magnetron Cathodes. Letter in Journal of Applied Physics. 21:1066-1067, October 1950.